

# Magnetic field-induced transition with spin rotation in the superconducting phase of $\text{UTe}_2$

K. Kinjo,<sup>1,\*</sup> H. Fujibayashi,<sup>1</sup> S. Kitagawa,<sup>1</sup> K. Ishida,<sup>1,†</sup> Y. Tokunaga,<sup>2</sup> H. Sakai,<sup>2</sup> S. Kambe,<sup>2</sup> A. Nakamura,<sup>3,4</sup>  
Y. Shimizu,<sup>3,4</sup> Y. Homma,<sup>3,4</sup> D. X. Li,<sup>3,4</sup> F. Honda,<sup>3,4</sup> D. Aoki,<sup>3,5</sup> K. Hiraki,<sup>6</sup> M. Kimata,<sup>7</sup> and T. Sasaki<sup>7</sup>

<sup>1</sup>Department of Physics, Graduate School of Science, Kyoto University, Kyoto 606-8502, Japan

<sup>2</sup>Advanced Science Research Center, Japan Atomic Energy Agency, Tokai, Ibaraki 319-1195, Japan

<sup>3</sup>Institute for Materials Research, Tohoku University, Oarai, Ibaraki 311-1313, Japan

<sup>4</sup>Central Institute of Radioisotope Science and Safety, Kyushu University, Fukuoka 819-0395, Japan

<sup>5</sup>Université Grenoble Alpes, CEA, IRIG, PHELIQS, F-38000 Grenoble, France

<sup>6</sup>Department of Physics, Fukushima Medical University, Fukushima 960-1295, Japan

<sup>7</sup>Institute for Materials Research, Tohoku University, Sendai 980-8577, Japan

(Dated: June 8, 2022)

$\text{UTe}_2$  is a recently discovered spin-triplet superconductor. One of the characteristic features of  $\text{UTe}_2$  is a magnetic field ( $H$ )-boosted superconductivity above 16 T when  $H$  is applied exactly parallel to the  $b$  axis. To date, this superconducting (SC) state has not been thoroughly investigated, and the SC properties as well as the spin state of this high- $H$  SC (HHSC) phase are not well understood. In this study, we performed AC magnetic susceptibility and nuclear magnetic resonance (NMR) measurements and found that, up to 24.8 T, the HHSC state is intrinsic to  $\text{UTe}_2$  and quite sensitive to the  $H$  angle, and that its SC character is different from that in the low- $H$  SC (LHSC) state. The dominant spin component of the spin-triplet pair is along the  $a$  axis in the LHSC state but is changed in the HHSC state along the  $b$  axis. Our results indicate that  $H$ -induced multiple SC states originate from the remaining spin degrees of freedom.

Superconductivity occurs when a coherent quantum fluid is formed from electron pairs. For most superconductors, although the total spin ( $S$ ) of the pairs is in the singlet state ( $S = 0$ ), it is also possible in the triplet state ( $S = 1$ ). Such superconductors, called “spin-triplet superconductors,” are coherent quantum fluids with spin and orbital degrees of freedom. This superconducting (SC) state involves rich physics, including the application to “qubits” in quantum computers[1, 2]. However, spin-triplet superconductors are rare. Therefore, the nature of the spin-triplet pairing state was initially studied by analyzing the superfluidity of  $^3\text{He}$  [3, 4]. The recent discovery of ferromagnetic (FM) superconductors[5–7] has made it possible to study the spin-triplet pairing state in the superconductors. Additionally, a spin-triplet SC candidate  $\text{UTe}_2$  has been newly discovered[8]; the SC transition temperature  $T_c$  is 1.6  $\sim$  2.0 K[9, 10]. Although  $\text{UTe}_2$  undergoes no FM transition, it was considered to be an end member of FM superconductors owing to its physical similarity to FM superconductors[8, 9].

The results of the nuclear magnetic resonance (NMR) Knight-shift ( $K$ ) measurements to superconductors have provided important information about the spin state in the SC state[11, 12]. However, in FM superconductors, such information is obscured because of the internal field produced by FM ordered moments. Thus,  $\text{UTe}_2$  provides a special opportunity for studying spin-triplet physics because the lack of FM moments means that precise  $K$  measurements can be obtained.

The possible SC symmetry and irreducible representation of spin-triplet superconductivity in a  $D_{2h}$  point group corresponding to the orthorhombic crystal struc-

ture of  $\text{UTe}_2$  in the zero field and  $H \parallel b$  are listed in Table I and Table II [9, 13].

TABLE I. Classification of the odd-parity SC order parameters for point groups with  $D_{2h}$  in a zero field. The irreducible representation (IR) and its basis functions are listed. The dominant spin component in the SC state is also shown.

$D_{2h}$ (zero field)		
IR	Basis functions	SC spin comp.
$A_u$	$k_a \hat{a}, k_b \hat{b}, k_c \hat{c}$	
$B_{1u}$	$k_b \hat{a}, k_a \hat{b}$	$c$
$B_{2u}$	$k_a \hat{c}, k_c \hat{a}$	$b$
$B_{3u}$	$k_c \hat{b}, k_b \hat{c}$	$a$

TABLE II. Classification of odd-parity SC phases occurring in  $\text{UTe}_2$  under a  $b$ -axis magnetic field. The typical order parameters belonging to each IR are listed in Table 1.

IR of $C_{2h}$ (under field)		
$H$ direction	$A_u^{H \parallel b}$	$B_u^{H \parallel b}$
$H \parallel b$	$A_u + iB_{2u}$	$B_{3u} + iB_{1u}$

As a result of performing the  $K$  measurements under low external fields, we found that  $\text{UTe}_2$  is a spin-triplet superconductor with spin degrees of freedom. The important aspect to be clarified is the behavior of the remaining spin degrees under various experimental conditions, such as the application of a magnetic field and/or pressure.

The upper critical field of superconductivity ( $H_{c2}$ ) is strongly directionally dependent[14, 15]. When  $H$  was perfectly aligned along the  $b$  axis,  $H$ -boosted superconductivity was observed up to  $\sim 35$  T [8, 14–17]. The use of microscopic measurements to investigate this high- $H$  SC (HHSC) state is critical to understanding the nature of spin-triplet superconductivity, as well as the SC mechanism of  $\text{UTe}_2$ .

A  $^{125}\text{Te}$ -enriched single crystal  $5 \times 3 \times 1$  mm<sup>3</sup> in size, and with  $T_c \sim 1.65$  K, was prepared by applying a chemical vapor transport method. Figure 1(a) shows the  $^{125}\text{Te}$ -NMR spectra for  $H \parallel b$ , which are plotted against  $K = (f - f_0)/f_0$ . Here,  $f$  is the NMR frequency and  $f_0$  is the reference frequency determined as  $f_0 = (^{125}\gamma_n/2\pi)\mu_0 H$  with a  $^{125}\text{Te}$ -nuclear gyromagnetic ratio  $^{125}\gamma_n/2\pi = 13.454$  MHz/T. As shown in Fig. 1(b), there are two crystallographically inequivalent Te sites,  $4j$  and  $4h$ , with the point symmetries  $mm2$  and  $m2m$  in  $\text{UTe}_2$ ; these point symmetries are denoted as Te1 and Te2 sites, respectively. Correspondingly, we observed two  $^{125}\text{Te}$  NMR peaks, as has been reported previously [18]. An NMR peak with a smaller [larger]  $K$  in  $H \parallel b$  was assigned as a Te(1) [Te(2)] peak, in accordance with a previous study [18, 19]. For the accurate alignment of the sample, we utilized the Te(1) NMR shift as an angle marker and an NMR probe with a two-axis rotator. The two angles  $\theta$  and  $\phi$  have been defined as shown in Fig 1(c); the sample orientation was adjusted by tuning  $\theta$  and  $\phi$  such that the Te(1) shift became the minimum value, as shown in Fig. 1(d) and (e). The accuracy of the alignment was estimated to be  $\pm 0.2^\circ$  for  $\theta$  and  $\pm 0.5^\circ$  for  $\phi$ , where  $\theta$  ( $\phi$ ) is the angle between the  $b$  and  $a$  ( $c$ ) axes.

To confirm the SC phase diagram, we measured the radio frequency (RF) reflection coefficient for the NMR tank  $LC$  circuit using a vector network analyzer, where  $L$  and  $C$  are the inductance and capacitance, respectively.  $\nu_{\text{tune}} \sim 1/\sqrt{LC}$  is a good measure for tracking the superconductivity, because the inductance of the NMR coil with the sample, i.e.,  $L = L_0(1 + q\chi_{\text{AC}})$ , where  $q$  is the ‘‘filling factor,’’ changes at the SC onset. Thus, the change in AC susceptibility ( $\chi_{\text{AC}}$ ) due to SC diamagnetism can be detected *in situ* by measuring the change in  $\nu_{\text{tune}}$  across  $T_c$  or  $H_{c2}$ .

Figure 2(a) shows the variation in  $-\Delta\nu/\nu_{\text{tune}}$ , as measured by sweeping  $H$  at 1.5, 1.0, and 0.6 K. At 1.5 and 1.0 K, the SC transitions were indicated by sudden decreases in the fields, as shown by the arrows. Although  $\text{UTe}_2$  is in the SC state at 0.6 K,  $-\Delta\nu/\nu_{\text{tune}}$  was found to exhibit a characteristic  $H$  dependence. Increasing  $H$  above 14 T corresponded to sharp decreases in  $|\Delta\nu/\nu_{\text{tune}}|$ ; however, further increase beyond 16.5 T coincided with increasing  $|\Delta\nu/\nu_{\text{tune}}|$ , indicating a kink at  $H_{\text{kink}} \sim 16.5$  T. Figure 2(b) shows the  $T$  dependence of  $-\Delta\nu/\nu_{\text{tune}}$  for  $\mu_0 H = 7.5, 15.5, 16.5,$  and 24 T on cooling.

The minimum value of  $|\Delta\nu/\nu_{\text{tune}}|$ , in relation to SC diamagnetism, was observed at 16 T, consequently

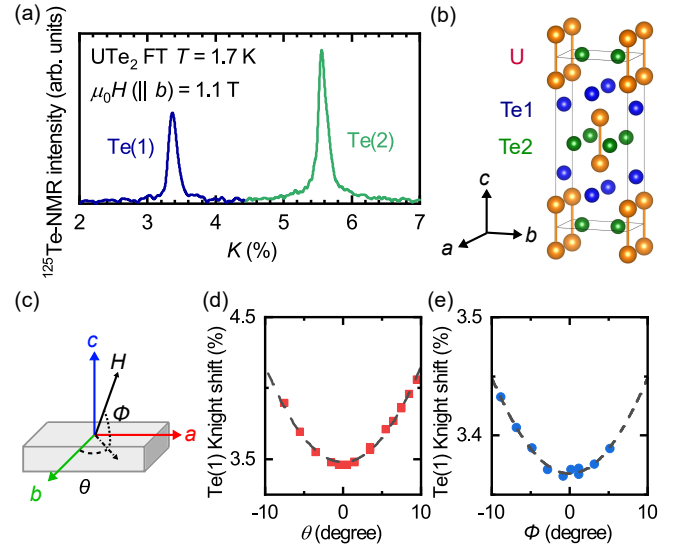


FIG. 1. (a)  $^{125}\text{Te}$ -NMR spectra measured in  $H \parallel b$ . A NMR peak with the smaller [larger]  $K$  is called Te(1) [Te(2)] in this paper. (b) The crystal structure of  $\text{UTe}_2$ [20]. There are two Te sites in  $\text{UTe}_2$ . (c) Definition of the angles  $\theta$  and  $\phi$  against the crystalline axes in  $\text{UTe}_2$  (d), [(e)] The  $\theta$  [ $\phi$ ] dependence of the  $K$  in the Te(1) peak. The  $b$  axis [ $(\theta, \phi) = (0, 0)$ ] is determined from the minimum of  $K$  at the Te(1) site.

demonstrating the same tendency as  $T_c$ . This indicates that the HHSC state is intrinsic to  $\text{UTe}_2$ . The  $H$  and  $T$  dependencies of  $-\Delta\nu/\nu_{\text{tune}}$  suggest that the SC character changed at  $\mu_0 H_{\text{kink}} \sim 16.5$  T. In fact, the HHSC state was found to be very sensitive to the angle  $\theta$ . Additionally, superconductivity was observed within  $\pm 3^\circ$  at 24 T, as shown in Fig. 2(c), and the unexpected minute  $\theta$  rotation ( $\Delta\theta \sim 4^\circ$ ) that occurred during the experiments completely suppressed the high- $H$  superconductivity, although the SC diamagnetism in the low- $H$  SC (LHSC) state was nearly unchanged, as shown by the dotted curve in Fig. 2(a). This result is in agreement with the results presented in previous reports[14, 15]. Based on the  $T$ - and  $H$ -scan measurements of  $-\Delta\nu/\nu_{\text{tune}}$ , we developed the SC  $H_{c2}$  phase diagram shown in Fig. 2(d). The  $H_{\text{kink}}$  anomaly, like the overall phase diagram, is consistent with the phase transitions determined by the recent specific-heat measurements[21]. Because the responses to  $H$  and  $\theta$  are different between the LHSC and HHSC states, it is reasonable to consider that the kink at  $H_{\text{kink}}$  marks a phase transition between the two SC states. Such a transition between two bulk SC states was also confirmed in the work[21] by linear magnetostriction and thermal dilatation, evidencing anomalies due to vortex pinning in both phases. The results of the  $H$ -sweep measurement at 0.6 K revealed clear hysteresis behavior at  $\mu_0 H^* \sim 4$  T; it was found to be related to an anomaly of the vortex state, because the anomaly was not previously observed in the  $H$  dependence results for the

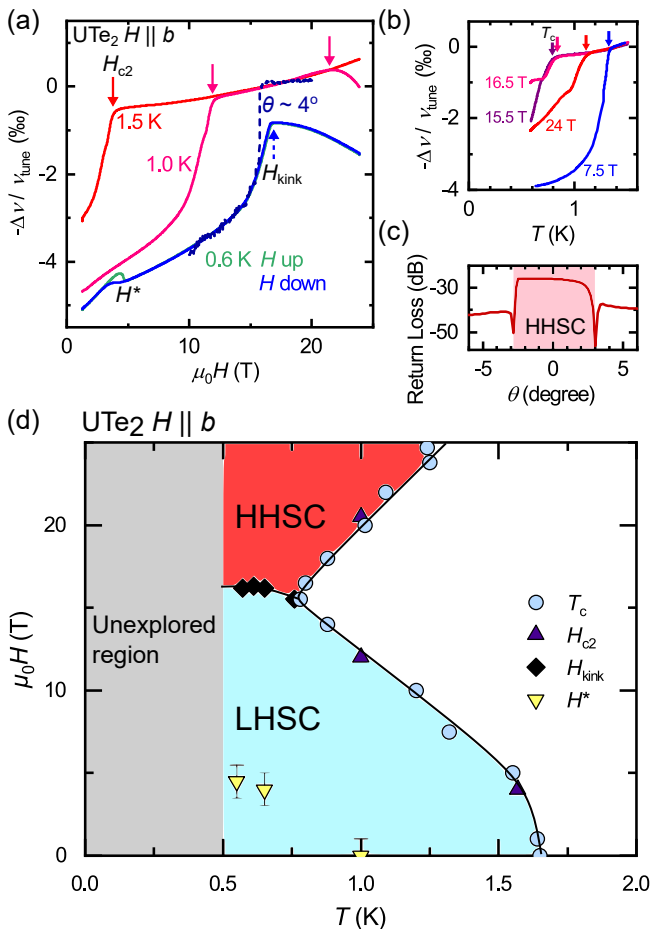


FIG. 2. (a)  $H$  dependence of  $-\Delta\nu/\nu_{\text{tune}}$  values up to 24.8 T, as measured at 0.6, 1.0 and 1.5 K. At 0.6 K,  $-\Delta\nu/\nu_{\text{tune}}$  exhibited a kink at  $H_{\text{kink}}$ ; the  $H$  dependence of  $-\Delta\nu/\nu_{\text{tune}}$ , which was determined by performing  $H$ -up and  $H$ -down sweeps, is shown. The dotted curve shows the  $H$  dependence of  $-\Delta\nu/\nu_{\text{tune}}$  when the minute  $\theta$  rotation unexpectedly occurred in the sample. (b) Temperature dependence of  $-\Delta\nu/\nu_{\text{tune}}$  in relation to the AC magnetic susceptibility  $\chi_{\text{AC}}$ , as measured at 7.5, 15.5, 16.5, and 24 T.  $T_c$  in the field is denoted by the arrow with the same color. (c) Angle dependence of the return loss of the NMR tank circuit at 24 T. When the sample was in the SC state, the quality factor of the circuit  $Q$  was lower owing to the change in the impedance of the circuit. High- $H$  superconductivity was observable within  $\pm 3^\circ$ . (d) SC upper critical field  $H_{c2}$  determined by performing  $T$ - and  $H$ -scan measurements of  $-\Delta\nu/\nu_{\text{tune}}$ .

electronic term in specific-heat measurements[22]. The details of this anomaly have been studied and will be reported in a separate paper.

To investigate the SC properties, particularly the spin susceptibility in the HHSC state, we performed  $^{125}\text{Te}$  NMR measurements at the Te(2) peak with a larger  $K$ . Figures 3(a) and (b) show the Te(2) NMR spectra measured at various temperatures below 2.5 K at 1 and 24 T, respectively. At 1 T, the single-peak spectrum grad-

ually shifted to the low- $K$  side in the normal state and sharply shifted immediately below  $T_c$ ; this was accompanied by spectrum broadening. The  $^{125}\text{Te}$  NMR spectrum measured under conditions of 24 T and 2.5 K revealed a double-peak structure that is attributable to its high resolution; the right peak was found to have a 0.04 % larger  $K$  than the main peak. Several possibilities were considered for the origin of the larger- $K$  peak; they include the occurrence of a mosaic structure and/or minute U-atom deficiency in the single-crystal sample. In the former case, the misalignment of the mosaic was estimated to be  $0.03^\circ$  ( $0.15^\circ$ ) on the  $a$  ( $c$ ) axis; additionally, the  $^{125}\text{Te}$  NMR measurement for the higher- $T_c$  single crystal is critical for the latter possibility because  $T_c$  seems to be very sensitive to a U-atom deficiency[9, 10, 23]. Further experiments are required to clarify the origin of the larger  $K$  peak.

As  $T$  was decreased, the two peaks gradually shifted to the lower- $K$  side in the same manner. Because the resolution of the higher- $K$  peak is not sufficient for analysis, we focus on the main peak shown by the arrows.

Figure 3(c) shows the temperature dependence of  $K$ , as determined from the peaks of the NMR spectra measured at 1, 10, 15, 20, and 24 T. A decrease in  $K$  was clearly observed at  $T_c$  for 1 and 10 T; the magnitude and  $H$  dependence of the  $K$  decrease below  $T_c$  are in agreement with previous results[19, 24]. In contrast, when 20 and 24 T were applied,  $K$  gradually decreased at temperatures below 2.5 K without any appreciable anomaly at  $T_c(H)$ . To quantify the Knight-shift decrease ( $\Delta K$ ) ascribed to the superconductivity, the normal-state  $T$  dependence was subtracted from the observed  $K_b$  and  $\Delta K$  was plotted for each  $H$ , as shown in the inset of Fig. 3(c). It is noteworthy that  $\Delta K$  was near zero in the SC state for values above 15 T. A similar  $\Delta K \sim 0$  trend was previously observed in  $a$ -axis Knight-shift measurement results for the LHSC state, where the dominant SC spin component occurred along the  $a$  axis [25]. Thus, these results indicate that  $b$ -axis spin-polarized superconductivity is induced by a  $b$ -axis magnetic field.

We will now discuss possible SC states in the HHSC region. Considering the observed spin-susceptibility and field-boosted behavior, the ground state of the HHSC is  $A_u^{H\parallel b}$ , as presented in table II; this is because the SC spin component is parallel to  $H \parallel b$  in the HHSC region. The kink anomaly in the field dependence  $-\Delta\nu/\nu_{\text{tune}}$  implies a phase transition between the HHSC and LHSC states; thus, the LHSC state is determined to be  $B_u^{H\parallel b}$ . These results strongly support the  $B_{3u}$  scenario at a low-field limit[19, 24–26]. Note that, in consideration of the related theories, we expected a first-order transition or two second-order transitions against  $H$  variation [13]. However, the results of the crude up-down  $H$ -sweep measurement of  $-\Delta\nu/\nu_{\text{tune}}$  at 0.6 K revealed the occurrence of one kink without any hysteresis near  $H_{\text{kink}}$ [Fig. 2(b)];

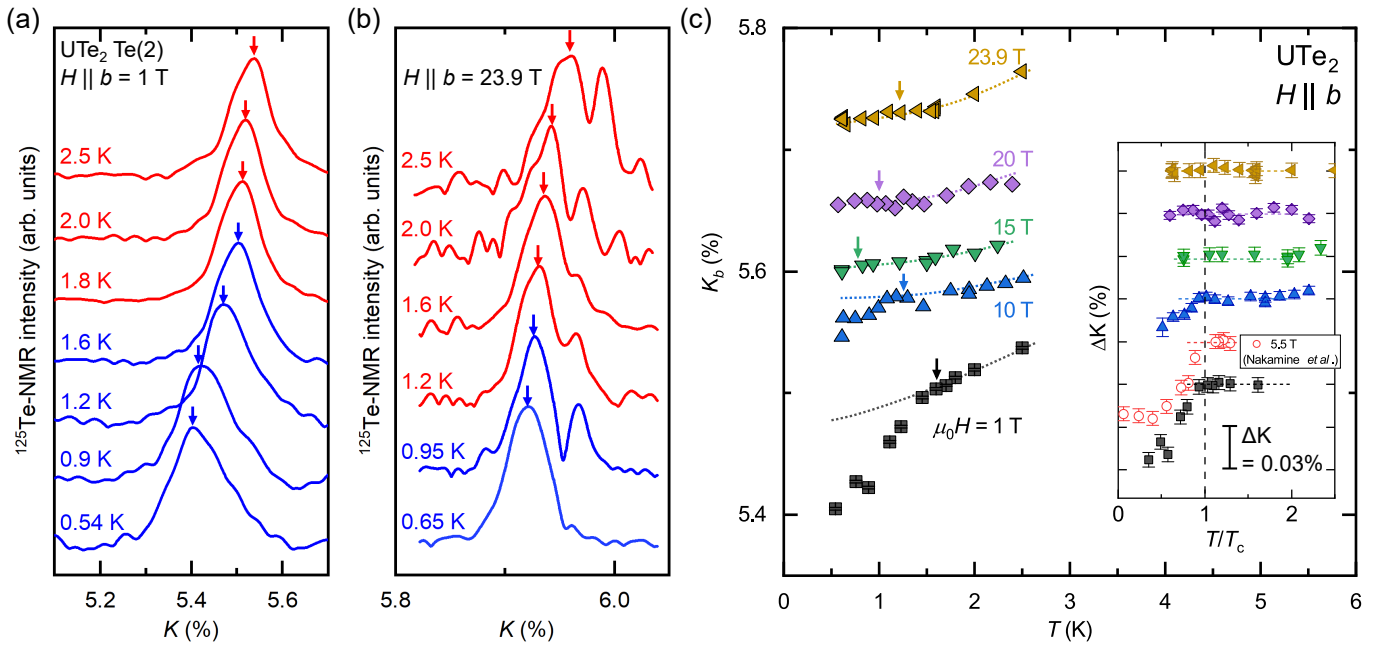


FIG. 3. Te(2) NMR peaks measured at various temperatures below 2.5 K at  $\sim 1$  T (a) and  $\sim 24$  T (b). (c) Temperature dependence of  $K$ , as determined by analyzing the Te(2) NMR peak shown by the arrow. The dotted line is the normal-state behavior extrapolated using the 2nd-order polynomial function as explained in the supplemental materials. (inset) Temperature dependence of the change in the Knight shift from the normal state. The temperature dependence of the normal-state Knight shift was fitted and subtracted using a quadratic function. The horizontal dashed line represents the baseline, and the vertical dashed line represents the transition temperature.

thus, the physical properties of the phase transition are inconclusive. Further precise measurements are required to determine the thermodynamic properties of this phase transition.

In addition, it is noteworthy that the enhancement of the superconductivity against  $H$  was found to be stronger than that previously reported [8, 14, 17]. Because the value of  $T_c$  at  $H = 0$  for the current sample (1.64 K) was slightly higher than that of previous samples ( $\sim 1.5$  K), the upturn behavior is seemingly dependent on the sample quality, suggesting the intrinsic properties of  $\text{UTe}_2$ . A similar level of superconductivity robustness by  $H \parallel b$  was observed in the FM superconductors  $\text{URhGe}$ [27] and  $\text{UCoGe}$ [28], in which critical FM fluctuations were determined to play an important role [29–32]. Because superconductivity occurs in the paramagnetic state of  $\text{UTe}_2$ , such critical FM fluctuations were not anticipated. Alternatively, we speculate that the criticality of the short-range order stabilized at  $\sim 12$  K[33, 34], or the critical fluctuations related to the incommensurate antiferromagnetic fluctuations[35, 36], which may be induced by  $H \parallel b$  above 16.5 T, plays an important role in the mechanism governing the HHSC state. It is interesting that the SC pairing interaction can be tuned by adjusting the  $H$  applied along the  $b$  axis; this seems to be a common feature of U-based FM and nearly FM superconductors with Ising anisotropy under normal-state magnetic condi-

tions, although the SC pairing interaction is not clarified in  $\text{UTe}_2$ .

In conclusion, we have determined from the results of *in-situ*  $\chi_{AC}$  and NMR measurements at magnetic field strengths up to 24.8 T, that the HHSC state is intrinsic nature of  $\text{UTe}_2$ , and that the spin component of the triplet pair occurs along the  $b$  axis in the HHSC state, which is different from that in the LHSC state. The results presented here provide decisive evidence that the spin degrees in a spin-triplet pair can be controlled by an external magnetic field  $H$ . This is a unique phenomenon that is not expected in spin-singlet superconductors, but is inherent to spin-triplet superconductors. Exploring unique phenomena related to the spin degrees of freedom in spin-triplet superconductors is important because this information can facilitate their application to quantum computers. This study is currently in progress.

The authors thank Y. Yanase, K. Machida, S. Fujimoto, V. P. Mineev, Y. Maeno, S. Yonezawa, J-P. Brison, G., Knebel, and J. Flouquet for their valuable discussions. They would also like to thank K. Shirasaki and M. Nagai for their technical support and Editage (www.editage.com) for English-language editing. This work was performed at High Field Laboratory for Superconducting Materials (HFLSM) under the GIMRT program of the Institute for Materials Research (IMR), Tohoku University (Proposal

Nos. 202012-HMKPB-0012, 202112-IRKAC-0023, and 202112-HMKPB-0008). This work was supported by the Kyoto University LTM Center and Grants-in-Aid for Scientific Research (Grant Nos. JP19K03726, JP19K14657, JP19H04696, JP19H00646, JP20H00130, JP20KK0061, and 21K18600). This work was also supported by JST SPRING (Grant Number JPMJSP2110). Some authors would like to acknowledge the support from the Motizuki Fund of Yukawa Memorial Foundation.

\* kinjo.katsuki.63v@st.kyoto-u.ac.jp

† kishida@scphys.kyoto-u.ac.jp

- [1] A. Gulian and K. Wood, *IEEE Trans. Appl. Supercond.* **13**, 944 (2003).
- [2] M. Leijnse and K. Flensberg, *Phys. Rev. Lett.* **111** (2013).
- [3] D. D. Osheroff, R. C. Richardson, and D. M. Lee, *Phys. Rev. Lett.* **28**, 885 (1972).
- [4] A. J. Leggett, *Rev. Mod. Phys.* **47**, 331 (1975).
- [5] S. S. Saxena, P. Agarwal, K. Ahilan, F. M. Grosche, R. K. W. Haselwimmer, M. J. Steiner, E. Pugh, I. R. Walker, S. R. Julian, P. Monthoux, G. G. Lonzarich, A. Huxley, I. Sheikin, D. Braithwaite, and J. Flouquet, *Nature* **406**, 587 (2000).
- [6] D. Aoki, A. Huxley, E. Ressouche, D. Braithwaite, J. Flouquet, J. P. Brison, E. Lhotel, and C. Paulsen, *Nature* **413**, 613 (2001).
- [7] N. T. Huy, A. Gasparini, D. E. de Nijs, Y. Huang, J. C. P. Klaasse, T. Gortenmulder, A. de Visser, A. Hamann, T. Görlach, and H. v. Löhneysen, *Phys. Rev. Lett.* **99**, 067006 (2007).
- [8] S. Ran, C. Eckberg, Q.-P. Ding, Y. Furukawa, T. Metz, S. R. Saha, I.-L. Liu, M. Zic, H. Kim, J. Paglione, and N. P. Butch, *Science* **365**, 684 (2019).
- [9] D. Aoki, J.-P. Brison, J. Flouquet, K. Ishida, G. Knebel, Y. Tokunaga, and Y. Yanase, *J. Condens. Matter Phys.* **34**, 243002 (2022).
- [10] P. F. S. Rosa, A. Weiland, S. S. Fender, B. L. Scott, F. Ronning, J. D. Thompson, E. D. Bauer, and S. M. Thomas, *Commun. Mater.* **3**, 33 (2022).
- [11] K. Yosida, *Phys. Rev.* **106**, 893 (1957).
- [12] D. E. MacLaughlin, *Solid State Physics* (Elsevier, 1976) pp. 1–69.
- [13] J. Ishizuka, S. Sumita, A. Daido, and Y. Yanase, *Phys. Rev. Lett.* **123**, 217001 (2019).
- [14] G. Knebel, W. Knafo, A. Pourret, Q. Niu, M. Vališka, D. Braithwaite, G. Lapertot, M. Nardone, A. Zitouni, S. Mishra, I. Sheikin, G. Seyfarth, J.-P. Brison, D. Aoki, and J. Flouquet, *J. Phys. Soc. Jpn.* **88**, 063707 (2019).
- [15] S. Ran, I.-L. Liu, Y. S. Eo, D. J. Campbell, P. M. Neves, W. T. Fuhrman, S. R. Saha, C. Eckberg, H. Kim, D. Graf, F. Balakirev, J. Singleton, J. Paglione, and N. P. Butch, *Nat. Phys.* **15**, 1250 (2019).
- [16] A. Miyake, Y. Shimizu, Y. J. Sato, D. Li, A. Nakamura, Y. Homma, F. Honda, J. Flouquet, M. Tokunaga, and D. Aoki, *J. Phys. Soc. Jpn.* **88**, 063706 (2019).
- [17] W. Knafo, M. Nardone, M. Vališka, A. Zitouni, G. Laperot, D. Aoki, G. Knebel, and D. Braithwaite, *Commun. Phys.* **4** (2021).
- [18] Y. Tokunaga, H. Sakai, S. Kambe, T. Hattori, N. Higa, G. Nakamine, S. Kitagawa, K. Ishida, A. Nakamura, Y. Shimizu, Y. Homma, D. Li, F. Honda, and D. Aoki, *J. Phys. Soc. Jpn.* **88**, 073701 (2019).
- [19] G. Nakamine, K. Kinjo, S. Kitagawa, K. Ishida, Y. Tokunaga, H. Sakai, S. Kambe, A. Nakamura, Y. Shimizu, Y. Homma, D. Li, F. Honda, and D. Aoki, *Phys. Rev. B* **103**, L100503 (2021).
- [20] K. Momma and F. Izumi, *J. Appl. Crystallogr.* **44**, 1272 (2011).
- [21] A. Rosuel, C. Marcenat, G. Knebel, T. Klein, A. Pourret, N. Marquardt, Q. Niu, S. Rousseau, A. Demuer, G. Seyfarth, G. Lapertot, D. Aoki, D. Braithwaite, J. Flouquet, and J.-P. Brison, *arXiv:2205.04524* (2022).
- [22] S. Kittaka, Y. Shimizu, T. Sakakibara, A. Nakamura, D. Li, Y. Homma, F. Honda, D. Aoki, and K. Machida, *Phys. Rev. Research* **2**, 032014 (2020).
- [23] Y. Haga, P. Opletal, Y. Tokiwa, E. Yamamoto, Y. Tokunaga, S. Kambe, and H. Sakai, *Journal of Physics: Condensed Matter* **34**, 175601 (2022).
- [24] G. Nakamine, K. Kinjo, S. Kitagawa, K. Ishida, Y. Tokunaga, H. Sakai, S. Kambe, A. Nakamura, Y. Shimizu, Y. Homma, D. Li, F. Honda, and D. Aoki, *J. Phys. Soc. Jpn.* **90**, 064709 (2021).
- [25] H. Fujibayashi, G. Nakamine, K. Kinjo, S. Kitagawa, K. Ishida, Y. Tokunaga, H. Sakai, S. Kambe, A. Nakamura, Y. Shimizu, Y. Homma, D. Li, F. Honda, and D. Aoki, *J. Phys. Soc. Jpn.* **91** (2022).
- [26] G. Nakamine, S. Kitagawa, K. Ishida, Y. Tokunaga, H. Sakai, S. Kambe, A. Nakamura, Y. Shimizu, Y. Homma, D. Li, F. Honda, and D. Aoki, *J. Phys. Soc. Jpn.* **88**, 113703 (2019).
- [27] F. Levy, I. Sheikin, B. Grenier, and A. D. Huxley, *Science* **309**, 1343 (2005).
- [28] D. Aoki, T. D. Matsuda, V. Taufour, E. Hassinger, G. Knebel, and J. Flouquet, *J. Phys. Soc. Jpn.* **78**, 113709 (2009).
- [29] Y. Tokunaga, D. Aoki, H. Mayaffre, S. Krämer, M.-H. Julien, C. Berthier, M. Horvatić, H. Sakai, S. Kambe, and S. Araki, *Phys. Rev. Lett.* **114**, 216401 (2015).
- [30] T. Hattori, Y. Ihara, K. Karube, D. Sugimoto, K. Ishida, K. Deguchi, N. K. Sato, and T. Yamamura, *J. Phys. Soc. Jpn.* **83**, 061012 (2014).
- [31] B. Wu, G. Bastien, M. Taupin, C. Paulsen, L. Howald, D. Aoki, and J.-P. Brison, *Nat. Commun.* **8**, 14480 (2017).
- [32] K. Ishida, S. Matsuzaki, M. Manago, T. Hattori, S. Kitagawa, M. Hirata, T. Sasaki, and D. Aoki, *Phys. Rev. B* **104** (2021).
- [33] K. Willa, F. Hardy, D. Aoki, D. Li, P. Wiecki, G. Laperot, and C. Meingast, *Phys. Rev. B* **104** (2021).
- [34] Y. Tokunaga, H. Sakai, S. Kambe, Y. Haga, Y. Tokiwa, P. Opletal, H. Fujibayashi, K. Kinjo, S. Kitagawa, K. Ishida, A. Nakamura, Y. Shimizu, Y. Homma, D. Li, F. Honda, and D. Aoki, *J. Phys. Soc. Jpn.* **91** (2022).
- [35] C. Duan, K. Sasmal, M. B. Maple, A. Podlesnyak, J.-X. Zhu, Q. Si, and P. Dai, *Phys. Rev. Lett.* **125** (2020).
- [36] W. Knafo, G. Knebel, P. Steffens, K. Kaneko, A. Rosuel, J.-P. Brison, J. Flouquet, D. Aoki, G. Lapertot, and S. Raymond, *Phys. Rev. B* **104**, L100409 (2021).
- [37] D. Aoki, A. Nakamura, F. Honda, D. Li, Y. Homma, Y. Shimizu, Y. J. Sato, G. Knebel, J.-P. Brison, A. Pourret, D. Braithwaite, G. Lapertot, Q. Niu, M. Vališka, H. Harima, and J. Flouquet, *J. Phys. Soc. Jpn.* **88**,

043702 (2019).

# Supplemental information for “Magnetic field-induced transition with spin rotation in the superconducting phase of UTe<sub>2</sub>”

## EXPERIMENTS

### AC-susceptibility and NMR measurements.

<sup>125</sup>Te NMR measurements were performed under the conditions of a maximum magnetic field strength of 24 T and minimum temperature of 0.6 K using a 25-T cryogen-free SC magnet in the High-Field Laboratory for Superconducting Materials at the Institute for Materials Research at Tohoku University. The applied magnetic field was calibrated using a <sup>63/65</sup>Cu NMR signal from the Cu NMR coil. To precisely adjust the magnetic field applied to the *b* axis, the Te(1) NMR shift was used; this is because the *K* along the *b* axis at the Te(1) peak was found to be the lowest within the three-axis *K*; furthermore, the lowest *K* within the three axes has been reported to be more remarkable than that at the Te(2) site[18].

The resonant frequency of the NMR tank circuit was tuned at a frequency of  $\nu_{\text{tune}} \simeq 15$  MHz in the normal state, and the shift in the tuning frequency  $-\Delta\nu$  was monitored as a function of the temperature *T* and magnetic field *H*. At this frequency, the skin depth of the RF

current is estimated to be  $\sim 55\mu\text{ m}$  based on a residual resistivity of  $\sim 18.5\mu\Omega\text{ cm}$  for UTe<sub>2</sub> just above *T<sub>c</sub>*[8, 37]. Note that the return loss of the reflection coefficient is also a good measure, because the quality factor of the circuit “*Q*” is expressed as  $2\pi\nu_{\text{tune}}L/R$ .

**Subtracting the normal state value of *K*.** For determination of  $\Delta K$  in the inset of the Fig. 3(c), the normal state value was estimated by the second order polynomial function,

$$K_{\text{normal}}(T) = K_0 + A \times T + A \times T^2.$$

Then,  $\Delta K$  is calculated as follows,

$$\Delta K \equiv K(T) - K_{\text{normal}}(T).$$

When the superconductivity occurs with spin-polarization, the spin-susceptibility follows the normal-state behavior. Therefore,  $\Delta K$  represents the change of the spin-susceptibility only due to the superconductivity.